ISET Journal of Earthquake Technology, Paper No. 571, Vol. 59, No. 2, June 2022, pp. 47–71

EFFECT OF MULTIPLE EVENTS WITH NO REPAIRS ON DUCTILITY-BASED SEISMIC DESIGN

Hitanshu Sethi
Department of Civil Engineering, Indian Institute of Technology Kanpur
Kanpur 208016, E mail id: *sethihitanshu@gmail.com*

Vinay K. Gupta (Corresponding Author)
Department of Civil Engineering, Indian Institute of Technology Kanpur
Kanpur 208016, E mail id: *vinaykg@iitk.ac.in*

ABSTRACT

The current practice of designing for the most critical earthquake event expected during the design life of the structure does not account for the possibility of structure getting damaged due to the smaller events and being rendered unfit to survive the most critical event. This is particularly the case when no repairs are feasible after some or all of the smaller but damaging events. The safety of the structure in such cases may be ensured by suitably raising the design force level of the structure and thus by limiting the cumulative damage in the structure before the most critical event occurs. This study considers the estimation of required increase by modifying the concept of design force ratio (DFR) spectrum such that only the effects of multiplicity of events are taken into account. DFR represents the ratio of the design force level required for a given cumulative damage due to all events to that required for a given ductility demand during the most critical event. For more realistic estimates of the modified DFR, the existing formulation of estimating DFR spectrum is modified by generalizing the power spectral density function (PSDF)-based characterization of seismic hazard due to an event to apply for the oscillators of a wide range of damping ratios. The proposed 'representative PSDF' is based on suitably increasing the damping of the oscillator, depending on the definition of the strong-motion duration used. It is shown through a numerical study based on a hypothetical seismic region that the dependence of modified DFR on oscillator period may be ignored. Also, dependence on the sequence of events and on the directions of residual displacements is weak, and therefore, all residual displacements may be assumed in the same direction and all events may be assumed to occur in the increasing order of their damage-causing potential.

KEYWORDS: Ductility-Based Seismic Design; Multiple Events; Cumulative Damage; Modified Design Force Ratio Spectrum; Strong-Motion Duration; Generalized Spectrum-Compatible PSDF

INTRODUCTION

In the traditional seismic design philosophy a structure is so designed that it does not collapse during the most critical earthquake expected in the seismic region of the structure. The parameters of such an earthquake are estimated by using the information on past events in the seismic region of the structure and by considering the design life of the structure. It is thus implicitly assumed that the structure will be able to undergo vibrations during smaller events without undergoing significant damage before the occurrence of the most critical event. This may not always be true, however, as in the regions of moderate to large seismic activity, there may be several events which drive the structural response into the inelastic range and it may not be feasible to carry out repairs after some or all of these events. This is particularly so in the case of buildings in business districts where interruptions due to repairs may lead to huge financial losses. The cumulative damage due to all smaller events occurring before the most critical event may be significant enough to make the structure incapable of withstanding the most critical event. The cumulative damage may sometimes be so much that the structure becomes unusable, unless necessary repairs are carried out, or unserviceable for further use. The recent philosophy of performance-based seismic design (see, for example, Bozorgnia and Bertero [1]) ensures certain performance levels such that the structure may remain fit even after a moderate earthquake. However, in the absence of necessary repairs, the structure may still be unsafe for the most critical event. One possible solution to account for this scenario

is to explicitly consider the effects of multiplicity of damaging events and to suitably increase the design force level of the structure. The design force level may be so raised that the total damage caused by the events before the more critical event is small enough for the structure to withstand the most critical event without collapse, while no significant repairs are carried out in the structure after an event.

Quite a few studies have been carried out in the past to account for the effects of multiple earthquakes in seismic design. Elnashai et al. [2] showed that the deformation demand in the structure for a single event goes up significantly in the case of multiple events. Decanini et al. [3] discussed the effect of the multiple seismic events on the built architecture in Italy in the case of aftershocks. Amadio et al. [4] considered the effect of damage accumulation during multiple events by considering recorded ground motions and showed that compared to the single-degree-of-freedom (SDOF) models with hardening, strength decay and stiffness degradation, the elastic-perfectly-plastic oscillator was most vulnerable in the case of multiple events. In this study, ground motions during the multiple events were simulated by considering repetitions of identical accelerograms. In an attempt to simulate a more realistic seismic environment, Moustafa and Takewaki [5] considered a stochastic model for the repeated acceleration sequences. Hatzigeorgiou and Beskos [6] studied the inelastic displacement ratio of SDOF systems when those are subjected to repeated or multiple earthquake events. Hatzigeorgiou [7] showed that the multiple events have a significant effect on the displacement ductilty demand of a SDOF system compared to the design event. Hatzigeorgiou and Liolios [8] experimentally verified the damage accumulation in a structure without any retrofit and pointed out the effect of sequencing of events on the damage in the structure. Also, a method was proposed to calculate the ductility demand for multiple events by combining the ductility demands for the individual events.

While the above studies have clearly outlined the need of accounting for the effect of multiplicity of earthquake events in a seismic design, those have not been directed towards developing recommendations on how the traditional seismic design may be modified, particularly when repairs in between any two damaging events are not possible to be carried out. There are a few studies in which such efforts have been made. Das and Gupta [9] considered pre-designed reinforced concrete bare frames and identified those situations in which the yield force levels of these frames need to be raised in order to offset the additional damage due to aftershocks. Das et al. [10] developed a simple frequency-based methodology to estimate the design force ratio (DFR) spectrum for a given seismic environment in the case of elastic-perfectly plastic oscillators. Here, DFR represents the factor by which the design force level in the traditional seismic design of a SDOF structure should be raised such that the cumulative damage during the multiple earthquake events in its lifetime does not exceed a given level. Dey and Gupta [11] generalized the methodology of Das et al. [10] to account for non-negligible residual displacement after each event in the calculation of damage due to the event. It was shown that a conservative estimate of DFR spectrum would be obtained if the residual displacements after different events are assumed to be in same direction and if the most critical event occurs after all the smaller events have occurred. However, considering that DFR incorporates the effect of moving from conventional (ductility-based) design philosophy to damage-based design philosophy, along with the effect of multiplicity of earthquake events, DFR may not truly represent the modifications that may be required in the traditional design to account for the multiplicity of events. Further, the formulations of Das et al. [10] and Dey and Gupta [11] are based on power spectral density function (PSDF)-based characterization of the ground motion during an event and on the use of equivalent linear oscillator. The ground-motion characterizations in these studies need to be revisited because while it is convenient to use a spectrum-compatible PSDF, the damping of the equivalent linear oscillator depends on the level of inelastic response and therefore the use of a single PSDF (obtained from a single response spectrum) may not be realistic.

There are several ways in which the ground motion during an anticipated earthquake event may be characterized for the given site. A time-history based characterization becomes an obvious choice considering that the structure may behave nonlinearly in response to the ground motion. However, in view of the inherent uncertainty associated with a time-history based characterization, an ensemble of time-histories may have to be considered. Alternatively, the anticipated ground motion may be considered as a realization of the underlying ground motion process which is then characterized through its PSDF. In either of the two situations (i.e., time-history based and PSDF-based characterizations), it is a common practice to characterize the anticipated ground motion in the form of expected pseudo spectral acceleration (PSA) spectra of different damping ratios. The PSDF or time-histories are then obtained from the spectrum corresponding to the damping of the structure. Consequently, a lot of research in the past has been devoted to developing methods for generating the spectrum-compatible accelerograms and

spectrum-compatible PSDF. While the option of spectrum-compatible accelerograms is typically exercised for obtaining quantitatively meaningful response results, the option of using a spectrum-compatible PSDF is considered to be more convenient if the focus is on getting approximate and qualitatively correct response results.

Any PSDF-based characterization of ground acceleration processes has the inherent limitation of not being applicable to non-stationary processes. In a typical ground motion, both amplitude and frequency characteristics evolve with different types of seismic waves arriving at the site and continuous change taking place in the rate of energy arrival at the site, and thus a (time-independent) PSDF is not a realistic choice for characterizing a ground motion process. Only in a few cases where the stationary segment of the ground motion becomes very large compared to its entire duration, the Fourier amplitude spectrum and strong-motion duration of the motion can be used to define a reasonable PSDF for the underlying ground acceleration process. For example, Shrikhande and Gupta [12] and Das et al. [10] considered this definition of PSDF and sought to scale the so-obtained PSDF up/down by a constant such that the scaled PSDF leads to the specified peak ground acceleration (PGA) under the framework of stationary random vibration theory. Even in such cases, there are errors in the response calculations (carried out under the stationary random vibration theory with the help of the PSDF of the input excitation), particularly in the cases of lightly damped and/or flexible oscillators, since the PSDF of the response process is unable to account for the additional non-stationarity caused by the sudden application of the excitation; the response gets overestimated due to the excitation inherently assumed to be of infinite duration. Das et al. [10] tried to account for this non-stationarity by considering the transient transfer function evaluated at a fixed time instant within the duration of the excitation. It is however more common to consider an equivalent stationary ground motion process of specified duration and (fictitious) PSDF such that under the stationary random vibration theory, this process leads to a given response spectrum of certain damping ratio. The use of such a spectrum-compatible PSDF is considered to be quite convenient and accurate in the case of linear systems. However, there is no single well-accepted procedure to obtain a spectrum-compatible PSDF, and several different formulations have been proposed in the past (e.g., see Kaul [13]; Unruh and Kana [14]; Christian [15]; Gupta and Trifunac [16]). In each of these formulations, the computed spectrum-compatible PSDF is specific to the damping ratio of the response spectrum used and therefore the design spectra (characterizing seismic hazard for the same site) of two different damping ratios will lead to two different spectrum-compatible PSDFs. This becomes a serious limitation of these formulations when the PSDF is to be used with an oscillator of different damping ratio (than that of the parent design spectrum), e.g., in the case of an equivalent linear oscillator. Even though this problem has been addressed in the past by using the concept of 'envelope PSDF' (e.g., see Dey and Gupta [17]), a dedicated effort remains to be done to minimize the discrepancies between the PSDFs obtained from a given set of design spectra.

In this study, based on the thesis of the first author (Sethi [18]), it is proposed to modify the concept of DFR spectrum (Das et al. [10]) such that only the effects of multiplicity of events are taken into account, and thus the effects of shift from a conventional (ductility-based) design to damage-based design are excluded. It is assumed that on considering the damage state of collapse as the target cumulative damage in the structure, the modified spectrum will give the required raise in the design yield force level of a SDOF structure, for the structure to survive the most critical event even after the occurrence of smaller events expected during the design life of the structure when no repairs are carried out after those events. The frequency-based formulation of Dey and Gupta [11] is considered for estimating the modified DFR spectrum in the case of degrading elastic-perfectly-plastic oscillators. An attempt is made to modify this formulation such that the PSDF characterization considered therein is generalized for application to the oscillators of a wide range of damping ratios. Further, a sensitivity analysis is performed for the modified DFR spectrum to study the effects of various governing parameters like sequence of events, directions of residual displacements, ductility of the oscillator, and design life of the structure. The same hypothetical region of four faults is considered for this analysis as in Das et al. [10] and Dey and Gupta [11].

PROPOSED MODEL FOR PSDF CHARACTERIZATION OF EARTHQUAKE GROUND MOTION PROCESS

1. PSDF Characterization by Dey and Gupta [11]

Assuming the earthquake ground motion process to be weakly stationary over its strong-motion duration T_s and the strong-motion duration to be reasonably long, the (temporal) PSDF of the process may be approximated as

$$G(\omega) = \frac{|F(\omega)|^2}{\pi T_s} \tag{1}$$

where $F(\omega)$ denotes the Fourier spectrum of one of the realizations of the process. In the specific context of this study, $F(\omega)$ and T_s refer to the Fourier transform and strong-motion duration, as estimated for the perceived seismic hazard and $G(\omega)$ can be considered to represent the ensemble PSDF of the process. Das et al. [10] scaled $G(\omega)$ up/down uniformly so that the expected largest peak value corresponding to the scaled PSDF $\bar{G}(\omega)$ becomes same as the (estimated) PGA. This PSDF was meant to be used together with a transient transfer function evaluated at one-fifth the (estimated) strong-motion duration of the excitation.

Dey and Gupta [11] attempted to improve on the methodology of Das et al. [10] by (i) using the (estimated) pseudo spectral velocity (PSV) spectrum in place of $|F(\omega)|$ in Equation (1), and by (ii) modifying the calculated PSDF $G(\omega)$ such that the response of a set of single-degree-of-freedom oscillators with certain damping and varying periods corresponding to the scaled PSDF $\bar{G}(\omega)$ becomes same as an (estimated) response spectrum (for the same damping). This PSDF was meant to be used together with the steady-state transfer function of the oscillator. The concept of such a PSDF has been used earlier by Kaul [13], Unruh and Kana [14], Christian [15], Gupta and Trifunac [16] among various research workers. The details of the procedure used by Dey and Gupta [11] to modify $G(\omega)$ are given in Appendix I for the sake of completeness.

The (spectrum-compatible) PSDF obtained by Dey and Gupta [11] clearly depends on the damping ratio of the oscillators considered and should work for all the oscillators of that damping ratio which was considered in its calculation. In the linearization technique proposed by Caughey [19] and used by Das et al. [10] and Dey and Gupta [11], however, the damping ratio of the equivalent oscillator is more than that of the (nonlinear) oscillator considered (see Appendix II for details). Thus, $\bar{G}(\omega)$ estimated for the damping of the nonlinear oscillator will lead to an underestimation in the response of the equivalent linear oscillator, unless the variation in $\bar{G}(\omega)$ over different damping ratios is insignificant. To illustrate this, an example case of the S40E component of the ground motion recorded at McCabe School, El Centro Array #11 site during the 1979 Imperial Valley earthquake is considered. Figure 1 shows the PSDFs calculated for damping ratio ζ = 0.0, 0.02, 0.05, 0.1 and 0.2 from the PSV spectra of the ground motion (assuming those to be the 'expected' spectra). It is clearly observed that the five PSDFs are significantly different and thus we need to generalize $\bar{G}(\omega)$ for damage calculations such that this works across the oscillators of different damping ratios.

2. Proposed PSDF Characterization

The PSDFs calculated with the help of the steady-state transfer function of oscillator are strictly valid for the situations when the excitation acts for an infinite duration. Since the earthquake excitations occur for much less durations in comparison to the period of the oscillator for most oscillators, there is an underdevelopment of response. Caughey and Stumpf [20] have shown in the case of white noise excitations that the response of an oscillator takes time to develop fully and the maximum stationary value is not reached until a few cycles of vibration have taken place. The heavily-damped oscillators are able to achieve the peak response earlier than the lightly-damped oscillators. The underdevelopment of response leads to an artificial scaling down of the PSDF amplitudes when it is estimated from a response spectrum,

and since the extent of scaling down is more in the case of lightly damped systems, the (spectrum-compatible) PSDF amplitudes are greater for higher damping ratios (see Figure 1).

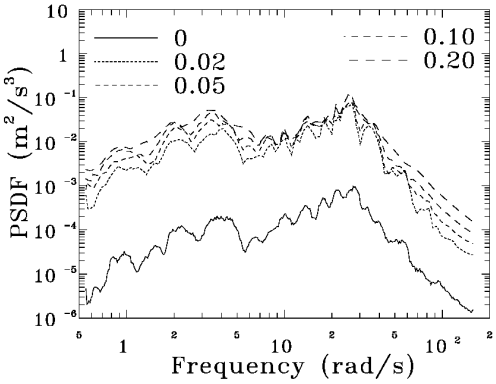

Fig. 1 Comparison of PSDFs calculated from the PSV spectra of the 1979 Imperial Valley earthquake motion for different damping ratios (as per the procedure used by Dey and Gupta [11])

The effect of finite operating time of the excitation leading to an underdevelopment of the oscillator response can be possibly accounted for by artificially increasing the damping of the oscillator as suggested by Rosenblueth and Elorduy [21]. Considering that the extent of underdevelopment will be more for flexible oscillators, this increase in damping should be more for flexible oscillators and shorter duration excitations. The use of increased damping in the calculation of a spectrum-compatible PSDF is thus less likely to render its dependence on the damping of the oscillators being considered. The concept of using increased damping in developing a spectrum-compatible PSDF is not new as it has been originally attempted by Unruh and Kana [14]. It is proposed to consider the following form of increased damping on the lines of the expression proposed by Rosenblueth and Elorduy [21]:

$$\tilde{\zeta} = \zeta + \alpha / \omega_n T \tag{2}$$

Here, ω_n is the natural frequency of the oscillator and T represents the strong-motion duration of the excitation. It may be noted that this expression becomes the same expression as proposed by Rosenblueth and Elorduy [21] for α = 2 and for T denoting the duration of a stationary process. Since Rosenblueth and Elorduy [21] did not propose any definition for T in the case of nonstationary processes like earthquake ground motion processes, it is proposed to consider various available definitions of strong-motion duration in the literature and to find a suitable value of α which will be consistent with the considered definition of strong-motion duration.

2.1 Strong-Motion Duration Definitions

Many definitions of duration are prevalent in literature for characterizing the strong-motion phase of a ground motion record and there is no consensus till date on which of these definitions can be considered as the most realistic definition in a variety of situations. In this study, following strong-motion durations are considered based on their greater acceptance in the earthquake engineering literature.

Bracketed Duration: This definition, first proposed by Ambraseys and Sarma [22], considered the time difference between the first and last excursions above a threshold limit. While this study considered a (fixed) threshold limit of 0.03 g (for all ground motions), this study considers a flexible threshold limit in terms of the peak ground acceleration (PGA) of the record as also considered earlier by Murphy and O'Brien [23]. This will ensure a fair treatment to the ground motions of widely varying PGAs. Five threshold limits, viz., 10%, 20%, 30%, 40%, 50% of the PGA, are considered and the corresponding definitions of strong-motion durations are denoted as TsBr10, TsBr20, TsBr30, TsBr40, TsBr50, respectively.

Uniform Duration: This definition was introduced by Sarma and Casey [24] in modification of the bracketed duration by considering all those time-intervals in which the threshold limit is exceeded and by adding their lengths. Although there is no single window of strong-motion phase in this definition, it is still considered as a possibility to characterize T for actual ground motions. Five threshold limits, viz.,

5%, 10%, 15%, 20%, 25% of the PGA, are considered and the corresponding duration definitions are denoted as TsUn05, TsUn10, TsUn15, TsUn20, TsUn25, respectively.

McCann-Shan Duration: McCann and Shah [25] related the root-mean square (rms) value of the acceleration to the strong-motion duration of excitation. The beginning of the strong-motion phase (at $t = T_1$) is defined as the instant beyond which the derivative of the cumulative rms value is always decreasing. The end of the strong-motion (at $t = T_2$) is assumed to be same as the beginning of the strong-motion phase in the case of the reversed record. The strong-motion duration is then given by $T_2 - T_1$. This definition of strong-motion duration is denoted here by TsMS.

Trifunac-Brady Duration: Trifunac and Brady [26] considered strong-motion duration to be the time-interval within which cumulative energy in the ground motion record varies from 5% to 95% of the total energy. This study considers the Trifunac-Brady duration in a generalized form by considering different levels of energy in the strong-motion segment of the motion, viz., 90%, 80%, 70%, 60% and 50% (of the total energy), and the resulting definitions are denoted as TsTB90, TsTB80, TsTB70, TsTB60 and TsTB50, respectively.

Vanmarcke-Lai Duration: Vanmarcke and Lai [27] also considered cumulative energy in the ground motion and proposed following expression for strong-motion duration in the case of accelerograms:

$$\text{TsVL} = 7.5 I_0 / a_{\max}^2 \tag{3}$$

where $a_{\max}$ denotes the PGA of the record and I_0 denotes the cumulative energy at the end of the record.

All definitions of strong-motion duration considered in this study for the value of T, together with their variants, are listed in Table 1.

Table 1: Details of strong-motion duration definitions considered

S. No.	Notation	Duration Definition	Threshold Limit
1	TsUn05	Uniform Duration	5% PGA
2	TsUn10	Uniform Duration	10% PGA
3	TsUn15	Uniform Duration	15% PGA
4	TsUn20	Uniform Duration	20% PGA
5	TsUn25	Uniform Duration	25% PGA
6	TsBr10	Bracketed Duration	10% PGA
7	TsBr20	Bracketed Duration	20% PGA
8	TsBr30	Bracketed Duration	30% PGA
9	TsBr40	Bracketed Duration	40% PGA
10	TsBr50	Bracketed Duration	50% PGA
11	TsTB90	Trifunac-Brady Duration	90% Seismic Energy
12	TsTB80	Trifunac-Brady Duration	80% Seismic Energy
13	TsTB70	Trifunac-Brady Duration	70% Seismic Energy
14	TsTB60	Trifunac-Brady Duration	60% Seismic Energy
15	TsTB50	Trifunac-Brady Duration	50% Seismic Energy
16	TsMS	McCann-Shah Duration	*Not Applicable*
17	TsVL	Vanmarcke-Lai Duration	*Not Applicable*

2.2 Estimation of α Value

Considering that (i) PSDF for a non-stationary process is a fictitious quantity, (ii) any strong-motion duration is only an approximate measure of the length of the strong-motion phase of the ground motion, and that (iii) response spectra (of different damping ratios) specified to characterize the seismic hazard at a site are not necessarily consistent with each other (i.e., there may be no single ground motion which will lead to the specified response spectra at the same time), there may be no single value of α for which PSDFs obtained from the spectra of different damping ratios are identical. Hence, for a given

strong-motion duration definition, a suitable value of α is proposed to be that value which leads to minimum variations in the PSDFs obtained from different spectra on considering the increased value of oscillator damping $\tilde{\zeta}$ instead of ζ.

Considering that the (effective) damping of the equivalent linear oscillator (Caughey [19]) for typically encountered structures may go up to 20%, the response spectra calculated for ζ = 0, 0.02, 0.05, 0.10 and 0.20 are considered in this study to obtain the (spectrum-compatible) PSDFs, and variations within those are sought to be minimized through the coefficient of variation (CoV) values computed at different frequencies. Figure 2 shows the variation of CoV with frequency for the PSDFs shown in Figure 1 (i.e., for α = 0) for the purpose of illustration. It is seen that the CoV values fluctuate between 0.55 and 1.05 and that the mean trend in the fluctuations varies slightly. Similar trends are observed for several other ground motions and for different values of α and definitions of T. For simplicity in the calculations, it is proposed to consider the averaged CoV across different frequencies as the representative CoV, referred to as MCoV hereafter, for the graph like the one in Figure 2 (for a given α, definition of T, and ground motion record). A higher value of MCoV would imply that the considered value of α for the considered definition of T leads to a significant variation in the PSDFs obtained for the response spectra of different damping ratios (of the ground motion record considered) and is thus unsuitable for characterizing a single PSDF corresponding to those response spectra.

It may be mentioned that MCoV will be estimated (for a given α, definition of T, and ground motion record) based on the (spectrum-compatible) PSDFs computed by following the same procedure as in Appendix I, but with the transfer function modified to

$$H_x(\omega) = \frac{-1}{\omega_n^2 - \omega^2 + 2\mathrm{i}\tilde{\zeta}\omega_n\omega} \tag{4}$$

and T_s taken same as T.

In order to find the most appropriate value of α for a given definition of T and ground motion record, MCoV is calculated for a range of α values starting from zero till the limiting value $\alpha_{\max}$ where

$$\alpha_{\max} = (1-\zeta)\omega_n T \tag{5}$$

corresponds to the maximum possible value of $\tilde{\zeta}$ = 1. Only the integer values of α are considered to reduce the level of computations, in view of the extensive computations required for various combinations of α, definition of T, and ground motion record. The intermediate values of MCoV are estimated from those for the integer values of α as discussed later in this section.

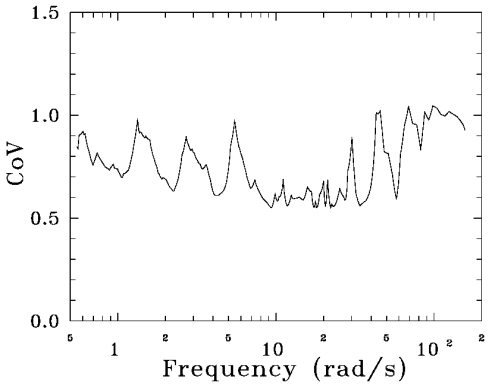

Fig. 2 Variation of CoV with frequency for the PSDFs shown in Figure 1

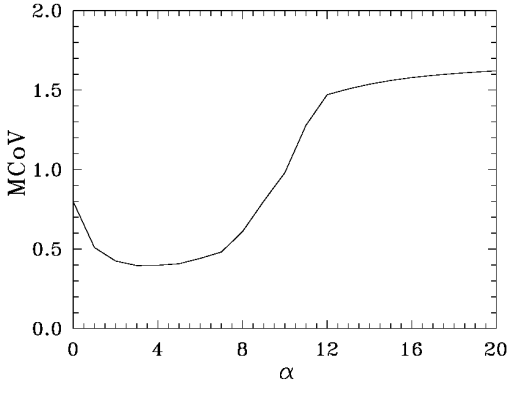

Fig. 3 Variation of MCoV with α for the TsTB90 strong-motion duration definition and 1954 Eureka earthquake motion

Figure 3 shows a typical variation of MCoV with (the integer values of) α, as obtained in the case of TsTB90 definition (of T) and N11W component of the ground motion recorded at the Eureka Federal Building site during the 1954 Eureka earthquake. It may be observed that as the value of α is increased

from zero, MCoV decreases to the minimum value of 0.4 around α = 3 and then increases monotonically for the higher values of α. While the minimum value of MCoV and the corresponding value of α depend on the ground motion record and the definition of T considered, the same trend is observed in all the cases. The existence of a minimum in the MCoV versus α curve is intuitively plausible because for a given ground motion record, there should be a right value of increase in damping which works more uniformly for different levels of damping ratios and thus the PSDFs obtained for different damping ratios approach a single PSDF. It is observed that an appropriate increase in damping may bring down the MCoV value from 0.8 (at α = 0, for no artificial increase in damping) to 0.4.

For a given definition of T, the MCoV versus α curve depends on the ground motion record and thus it is desirable to consider a large number of records to obtain a statistically meaningful value of α corresponding to that definition of T. A suite of 225 records listed in Sethi [18] is considered in this study. This suite is composed of (a) 205 ground motions considered by Samdaria and Gupta [28], and (b) 20 ground motions recorded during the 1994 Northridge earthquake. The first set of 205 accelerograms has been recorded during 36 earthquake events in western U.S.A between 1954 and 1984. All records have peak ground accelerations (PGAs) from 0.04 to 0.83 *g* and have (published) magnitudes *M* ranging from 3.2 to 6.6 (with $M \leq 5$ for 58 records, $5 < M \leq 6$ for 22 records, and $M > 6$ for 125 records) epicentral distances Δ up to 223 km (with $\Delta \leq 20$ km for 83 records, 20 km $< \Delta \leq 50$ km for 83 records, and $\Delta > 50$ km for 39 records), and site conditions from alluvium to rock (see Lee and Trifunac [29] for details). The second set of Northridge motions is listed in Table 2.

Table 2: Details of Northridge motions

Record No.	Name of Event	Component	Location of Recording Station
1	1994 Northridge Earthquake	East	Alhambra—Fremont School
2	1994 Northridge Earthquake	N72E	Los Angeles Dam
3	1994 Northridge Earthquake	S85W	Lower Franklin Dam
4	1994 Northridge Earthquake	East	Downey—County Maint. Bldg.
5	1994 Northridge Earthquake	W48N	Rinaldi Receiving Station
6	1994 Northridge Earthquake	N18E	Sylmar Converter Station-East
7	1994 Northridge Earthquake	N52E	Sylmar Converter Station
8	1994 Northridge Earthquake	East	Los Angeles—Baldwin Hills
9	1994 Northridge Earthquake	N90E	Hollywood Storage Grounds
10	1994 Northridge Earthquake	East	Malibu—Point Dume
11	1994 Northridge Earthquake	South	Moorpark
12	1994 Northridge Earthquake	N90E	Mt. Wilson
13	1994 Northridge Earthquake	East	Southwestern Academy
14	1994 Northridge Earthquake	S37E	624 Cypress Ave.
15	1994 Northridge Earthquake	N00W	8505 Saran Dr., Playa Del Rey
16	1994 Northridge Earthquake	S16W	Topanga Canyon Blvd., Canoga Park
17	1994 Northridge Earthquake	N08W	Angeles National Forest
18	1994 Northridge Earthquake	S90W	N. Holly Ave., Baldwin Park
19	1994 Northridge Earthquake	N90E	Briarcliff Dr., La Habra
20	1994 Northridge Earthquake	N30W	S. Seaside Ave., Terminal Island

As discussed above, different MCoV versus α curves are obtained for the 225 ground motion records considered for each of the 17 definitions of T (see Table 1). It will be logical to consider that value of MCoV to represent the performance of the definition of T at a given value of α which is exceeded for only a small number of records. The value of α at which this performance becomes the best, corresponding to the minimum value of so-calculated MCoV, may be considered to be an appropriate value of α for the definition of T considered. Alternatively, the minimum in the averaged MCoV versus α curves (across different ground motion records) may also be considered for simplicity. Figure 4 shows four averaged curves for the TsUn05, TsMS, TsTB90 and TsBr20 definitions (of T). These curves are smooth and hence the basic curve-fitting technique in the MATLAB functionality is used to obtain the points of minima in these curves (and the remaining 13 curves). Table 3 gives the values of α corresponding to the minima in average curves for the 17 definitions. The corresponding values of the minimized averaged MCoV are also given in this table.

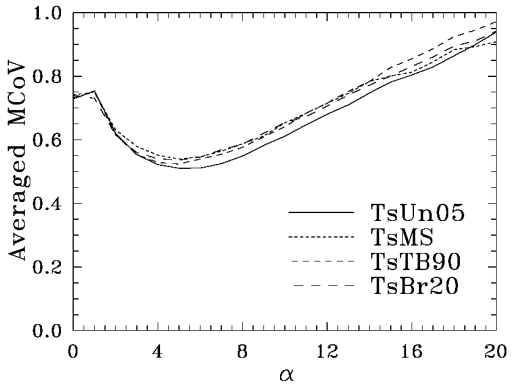

Fig. 4 Variations of averaged MCoV with α for different strong-motion duration definitions

Table 3: Values of α and corresponding averaged MCoV for different strong-motion duration definitions

S. No.	Duration Definition	α	Averaged MCoV
1	TsBr10	8.00	0.521
2	TsUn05	5.40	0.509
3	TsMS	5.30	0.540
4	TsTB90	4.70	0.523
5	TsBr20	4.80	0.535
6	TsUn10	3.00	0.519
7	TsTB80	3.00	0.536
8	TsBr30	3.00	0.541
9	TsVL	2.50	0.522
10	TsTB70	2.20	0.541
11	TsBr40	2.20	0.563
12	TsUn15	2.20	0.525
13	TsTB60	1.40	0.542
14	TsBr50	1.20	0.560
15	TsTB50	1.40	0.550
16	TsUn20	1.30	0.521
17	TsUn25	1.20	0.520

It may be observed that the values of α vary from 1.20 (for TsBr50 and TsUn25) to 8.0 (for TsBr10). The values of the minimized averaged MCoV vary from 0.509 (for TsUn05) to 0.563 (for TsBr40), and thus no definition is significantly better than the rest of the definitions. In view of this, it looks reasonable to stick to the well-known and used definitions of TsTB90, TsMS, TsUn05 and TsBr10. The values of α for these definitions are obtained as 4.7, 5.3, 5.4 and 8.0. Considering that the values of α vary little between the definitions of TsTB90, TsMS and TsUn05, for simplicity, it may be desirable to specify a uniform value of 5 for these three definitions. Further, the same value of α may be used if the TsBr20 variant of bracketed duration is to be used to define T. If one has to choose among the popular definitions, the definition of TsUn05 may be preferred due to its least 'minimum averaged MCoV'.

2.3 Representative PSDF

As discussed above, the use of increased damping (through the use of a non-zero α) leads to a significant reduction in the variability of the PSDFs obtained for different damping ratios. However, this does not become insignificant, and hence the role of damping in the spectrum-compatible PSDF does not get completely neutralized. This happens because (i) PSDF is a fictitious characterization of a nonstationary process, and (ii) the model used for increase in damping (see Equation (2)) is only an approximation. This problem may become more pronounced if the response spectra used are not

consistent with each other, as in the cases of the design spectra (of different damping ratios) specified by various codes of practice. To address this situation, a representative PSDF is proposed to be computed by taking the average of the five PSDFs obtained for a given set of response spectra (for different damping ratios), while assuming that those would be sufficient to cover the likely range of the damping ratios of the equivalent linear oscillators. This 'representative PSDF' may be used to characterize the ground motion process corresponding to the given set of spectra. Figure 5 shows such a representative PSDF for the S86W component of the ground motion recorded at the Santa Ana site during the 1968 Borrego Mountain Earthquake, obtained for use with the TsTB90 definition of T (with α = 5). The PSDF obtained via the method of Dey and Gupta [11] from the 5%-damping spectrum is also shown in the figure. It may be observed that as expected, the two curves overlap with each other at high frequencies, and at other frequencies, the representative PSDF is greater than the PSDF based on Dey and Gupta [11].

3. Comparison of Results

It will be interesting to see how the response of a nonlinear oscillator based on the (proposed) representative PSDF compares with that obtained (a) from the time-history analysis, and (b) in the formulations of Das et al. [10] and Dey and Gupta [11]. A comparative analysis is therefore performed by considering the maximum displacement and hysteretic energy responses of elastic-perfectly-plastic oscillators with the initial damping ratio of 5% and by estimating these responses for the four cases being compared. Damage is often defined as a linear combination of maximum displacement and hysteretic energy responses (see, for example, Park and Ang [30]), and therefore these responses may be of critical importance in the evaluation of damage potential of a ground motion. The oscillators considered have 97 periods ranging from 0.04 to 11.4 s such that those are equispaced on the logarithmic scale. The yield displacement levels of these oscillators are so chosen that the maximum displacement computed from the time-history analysis is three times the yield displacement in each of these cases (thus corresponding to the ductility demand of 3).

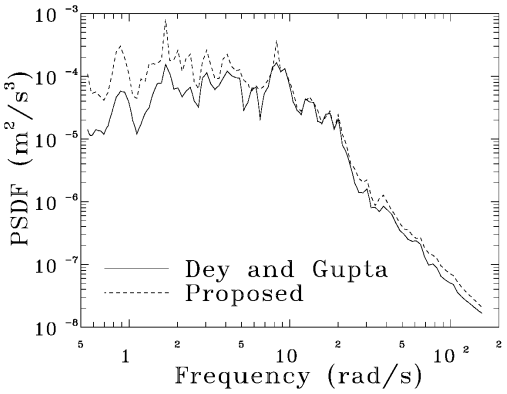

Fig. 5 Comparison of the proposed PSDF (for the TsTB90 strong-motion duration definition) and the PSDF from the procedure in Dey and Gupta [11] (for the 5%-damping PSV spectrum) for the 1968 Borrego Mountain earthquake motion

While a nonlinear time-history analysis is carried out to calculate the 'actual' peaks of oscillator displacement, PSDFs are estimated for the three approximate methods as in Sub-section 2.3 above. The approximate peaks of (nonlinear) oscillator displacement are estimated (for the representative PSDF and for the methods of Das et al. [10] and Dey and Gupta [11]) by considering the equivalent linear oscillators as in Caughey [19] (see Appendix II for details). The transfer function for the displacement response of the equivalent oscillator as in Equation (24) is however applicable only for the method of Dey and Gupta [11]. For the method of Das et al. [10], the transient transfer function evaluated at $t = T/5$ is used, and for the case of representative PSDF, Equation (24) is used with ζ_e replaced by $\zeta_e + \alpha / \omega_e T$. These alternative transfer functions are applicable (in the cases of Das et al. [10] and representative PSDF) both for the calculation of equivalent properties and for the determination of the response PSDF from the excitation PSDF. The second-order, third-order, and other higher-order expected displacement peaks (of the nonlinear oscillator) are obtained (for the estimation of hysteretic energy response) from the response PSDF by following the same approach as in Das et al. [10] and Dey and Gupta [11].

Figures 6–8 respectively show the comparisons of the (normalized) maximum displacement response for (a) the N11W component of the ground motion recorded at the Eureka Federal Building site during the 1954 Eureka earthquake, (b) the S86W component of the ground motion recorded at the Santa Ana site during the 1968 Borrego Mountain earthquake, and (c) the S40E component of the ground motion recorded at McCabe School, El Centro Array #11 site, during the 1979 Imperial Valley earthquake. Figures 9–11 show the comparisons of the (normalized) hysteretic energy response for the Eureka, Borrego Mountain and Imperial Valley motions, respectively. In each of Figures 6–11, the 'Actual' curves represent the time-history results, while the 'Proposed', 'Das', and 'Dey' curves respectively represent the approximate results corresponding to the proposed method and for the methods of Das et al. [10] and Dey and Gupta [11].

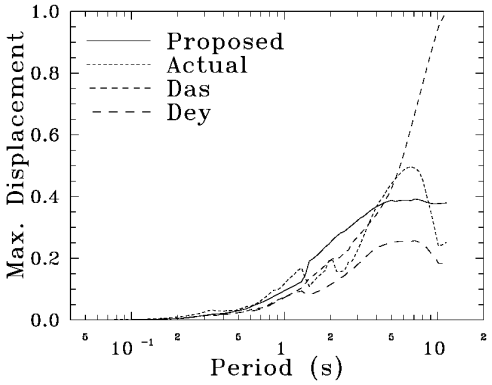

Fig. 6 Comparison of the 'Proposed', 'Das' and 'Dey' normalized maximum displacement spectra with the 'Actual' spectrum for the 1954 Eureka earthquake motion and ductility demand of 3

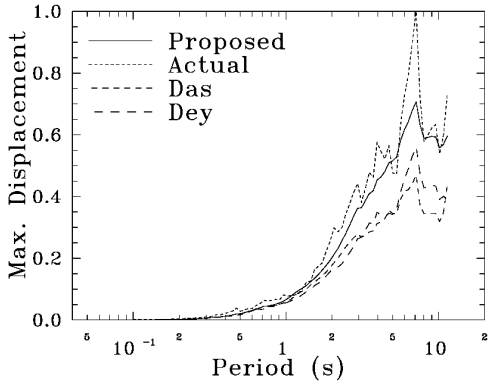

Fig. 7 Comparison of the 'Proposed', 'Das' and 'Dey' normalized maximum displacement spectra with the 'Actual' spectrum for the 1968 Borrego Mountain earthquake motion and ductility demand of 3

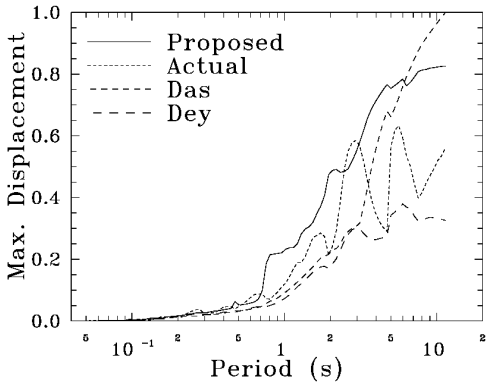

Fig. 8 Comparison of the 'Proposed', 'Das' and 'Dey' normalized maximum displacement spectra with the 'Actual' spectrum for the 1979 Imperial Valley earthquake motion and ductility demand of 3

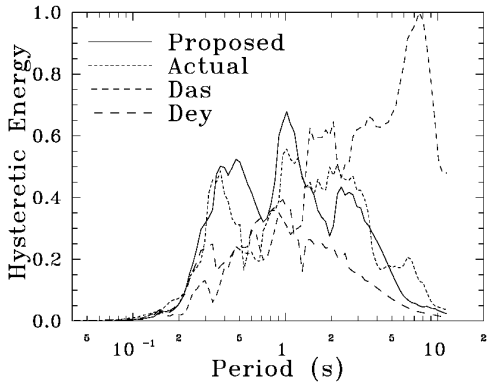

Fig. 9 Comparison of the 'Proposed', 'Das' and 'Dey' normalized hysteretic energy spectra with the 'Actual' spectrum for the 1954 Eureka earthquake motion and ductility demand of 3

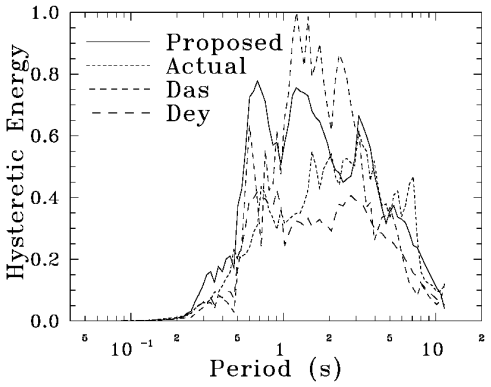

Fig. 10 Comparison of the 'Proposed', 'Das' and 'Dey' normalized hysteretic energy spectra with the 'Actual' spectrum for the 1968 Borrego Mountain earthquake motion and ductility demand of 3

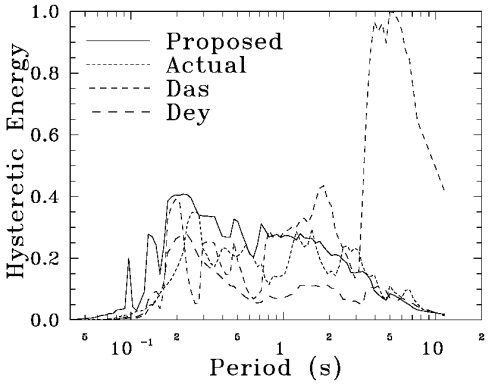

Fig. 11 Comparison of the 'Proposed', 'Das' and 'Dey' normalized hysteretic energy spectra with the 'Actual' spectrum for the 1979 Imperial Valley earthquake motion and ductility demand of 3

It may be observed from Figures 6–8 that the estimates of maximum displacement response from the proposed method have consistently good matching with the time-history estimates (with the rms error as 39.3%, 34.1%, and 60%, respectively). The estimates based on Dey and Gupta [11] are consistently lower due to increase in damping (on account of linearization) and the PSDF used being strictly applicable to 5% damping. However, the estimates based on Das et al. [10] have either good matching with the time-history estimates or are lower than those, except at long periods where the estimates based on Das et al. [10] may be significantly larger. Figures 9–11 also show almost similar trends as in Figures 6–8, with the estimates of the hysteretic energy from the proposed method being reasonably close to the time-history estimates and the estimates based on Das et al. [10] sometimes becoming too large at long periods (> 3 s). Thus, it appears that the (proposed) representative PSDF can be used together with the linearization scheme of Caughey [19] to reliably predict the nonlinear response of elastic-perfectly-plastic oscillators. This approach can be presumably made more effective by averaging the PSDFs for only those damping ratios that fall within the likely range of equivalent damping ratios (instead of the chosen values of 0, 0.02, 0.05, 0.10, and 0.20).

DUCTILITY-BASED DESIGN FOR MULTIPLICITY OF EVENTS

1. Modification in DFR Spectrum for Representative PSDF

Design force ratio (DFR) is defined as the ratio of the yield force level $\bar{Q}_y$ required to reach a specified level of cumulative damage in a SDOF system due to all seismic events expected to occur during the design life of the system, to the yield force level Q_y required for the ductility demand on the system during the most critical event to be same as the available ductility μ in the system (Das et al. [10]). For a given combination of available ductility, system damping, and target (cumulative) damage level, the DFR spectrum can be calculated for a given site in a given seismic environment. Appendix III briefly describes the procedure proposed by Dey and Gupta [11] for such calculations, under the conditions that no repairs are carried out in the system after any event and the effects of aftershocks are not included.

Dey and Gupta [11] considered the characterization of seismic hazard (at a site and due to an event during the design life of the system) by considering the power spectral density function (PSDF) compatible with the pseudo spectral acceleration (PSA) spectrum of the expected ground motion (due to the event under consideration) for the same damping as the given system damping (see Appendix III). It is proposed to replace this characterization by the representative-PSDF based characterization (as proposed in the previous section) via following modifications in the procedure of Dey and Gupta [11].

It is proposed to obtain (by using Equation (31)) five different descriptions of the PSDF $G_{lk}(\omega)$ (for the event of magnitude M_k occurring at the lth source) from the scaled PSV spectra, corresponding to the damping ratio ζ = 0%, 2%, 5%, 10% and 20%, and for the scaled strong-motion duration. Each of these descriptions is proposed to be modified to $\bar{G}_{lk}(\omega,\zeta)$ with the help of the PSA spectrum (as obtained from the scaled PSV spectrum of ζ damping ratio) by following the procedure of 'representative PSDF' proposed in the previous section, with α taken as 5 corresponding to the TsTB90 definition of strong-motion duration. The five different descriptions of $\bar{G}_{lk}(\omega,\zeta)$ (for ζ = 0%, 2%, 5%, 10%, and 20%) are averaged to obtain the representative PSDF $\bar{G}_{lk}(\omega)$ (for the event of magnitude M_k occurring at the lth source).

It may be mentioned that the representative-PSDF based characterization is associated with the use of a different transfer function for the displacement response of the equivalent oscillator from that used by Dey and Gupta [11]. Whereas Dey and Gupta [11] used Equation (24) for the calculation of the properties of the equivalent oscillator and for the determination of the response PSDF from the excitation PSDF, ζ_e in this equation needs to be replaced by $\zeta_e + \alpha/\omega_e T$ in the case of representative-PSDF based characterization, where T is same as the scaled strong-motion duration.

A numerical illustration of the use of representative-PSDF based characterization in the DFR spectrum calculations is carried out by considering the same case study as in Dey and Gupta [11]. A total of 17 elastic-perfectly-plastic oscillators are considered with the initial period T_n = 0.10, 0.15, 0.20, 0.25, 0.30, 0.40, 0.50, 0.60, 0.75, 0.90, 1.00, 1.10, 1.25, 1.50, 1.75, 2.00, and 2.50 s, damping ratio ζ = 0.05, and available ductility μ = 3, to represent the structure for which the DFR spectrum is to be calculated. The design life of the structure is taken as 50 yrs. The structure is considered to be located in a hypothetical area consisting of four nearby faults; two of them are located at a distance of 30 km from the site, while two others are located 40 km and 50 km away. The values of the constant a for these faults are 3.28, 4.03, 3.77, and 3.09, respectively, and the constant b is uniformly equal to 0.86 for all faults. The focal depths of all sources are uniformly equal to 5 km, and the area under consideration has alluvium geological site conditions. Only the earthquakes in the range from $M_{\min}$ = 5.0 to $M_{\max}$ = 8.0 are considered, thus leading to (a) 4 expected events of the magnitudes 6.03, 5.54, 5.24, and 5.13 for the first fault (with a = 3.28), (b) 26 expected events (with the largest magnitude of 6.84) for the second fault (with a = 4.03), (c) 14 expected events (with the largest magnitude of 6.57) for the third fault (with a = 3.77), and (d) 3 expected events (with the largest magnitude of 5.91) for the fourth fault (with a = 3.09). All the 47 events expected at the four faults are assumed to occur in the increasing order of their damage-causing potential, and the residual displacements for all of these events are assumed to be in the positive direction.

Figure 12 shows the DFR spectra for the target cumulative damage D = 0.8 (corresponding to the maximum possible damage without structural collapse) in the cases of the seismic hazard characterization by Dey and Gupta [11] and the representative-PSDF based characterization. It may be observed from the comparison of the two spectra that the representative-PSDF based characterization is associated with about 20% reduction compared to the DFR estimates of Dey and Gupta [11] at all periods and that both spectra show similar trends. These observations are also found to be applicable for the other combinations of residual displacement and sequence of events considered by Dey and Gupta [11].

2. Proposed DFR Spectrum for Multiplicity of Events

The design force ratio (DFR) proposed by Das et al. [10] may be expressed as

$$\alpha_R = \frac{\bar{Q}_y}{\hat{Q}_y} \times \frac{\hat{Q}_y}{Q_y} \tag{6}$$

where Q_y and $\bar{Q}_y$ are as defined above, and $\hat{Q}_y$ represents the yield force level required to reach a specified level of damage in a SDOF system because of the most critical event expected to occur during

its design life. Whereas $\bar{Q}_y$ corresponds to a damage-based design for multiple events, Q_y corresponds to a ductility-based design for single event and $\hat{Q}_y$ to a damage-based design for single event. Thus, the first ratio on the right-hand side of Equation (6) describes the effect of the multiplicity of events and the second ratio describes the effect of the shift from ductility-based design to damage-based design. Accordingly, α_R may be expressed as

$$\alpha_R = \alpha_{RM} \times \alpha_{RD} \tag{7}$$

where α_{RM} (= $\bar{Q}_y / \hat{Q}_y$) represents the effect of multiplicity of events on the yield force level and α_{RD} (= $\hat{Q}_y / Q_y$) the effect of the change in design philosophy. The ratio α_{RM} may be a better representative of a conventional design becoming unsafe, when the structure is subjected to several events during its design life and some of those events (other than the largest event) cause inelastic response in the structure. It is therefore proposed to consider the (modified) DFR spectrum for the multiplicity of events, describing the variation of α_{RM} with the initial period of the SDOF system for the given target cumulative damage level D (and ductility capacity of the system), and to study this spectrum for several possible variations in the governing parameters and underlying assumptions. For this purpose, $\bar{Q}_y$ is calculated as in Dey and Gupta [11] (along with the modifications proposed in Sub-section 1 above) for the damage index D, and $\hat{Q}_y$ is calculated for the largest of $\hat{D}_i$ = 1, 2, ..., n_e (instead of the summation) to become equal to D, where $\hat{D}_i$ denotes the damage in the system during the i th event (see Appendix III for further details) and n_e the total number of events expected during the lifetime of the system.

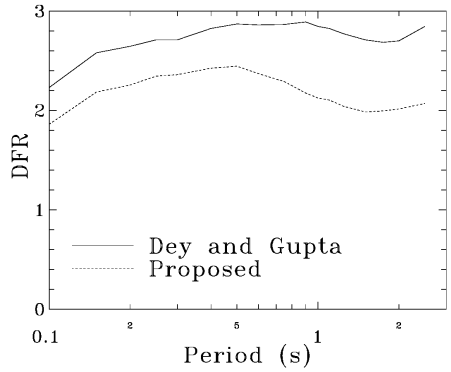

Fig. 12 Comparison of DFR spectra for the seismic hazard characterization by Dey and Gupta [11] and the 'Proposed' (representative PSDF based) characterization for maximum damage without collapse

Both $\hat{Q}_y$ and $\bar{Q}_y$ are obtained iteratively for an oscillator of given damping ratio, available ductility, target (cumulative) damage, and for a given seismic environment by following the steps given below:

(a) Estimate the magnitudes of the events expected on each fault of the given region (see Appendix III).

(b) Characterize ground motion for each of the expected events through the representative PSDF (see Sub-section 2.3 of the previous section), which is obtained from the PSDFs compatible with a given set of design spectra for different damping ratios (see Appendix I), while using the increased damping ratio from Equation (2) (instead of the damping ratio of the design spectrum). In this study, the design spectra used correspond to Equation (32) and the strong-motion durations correspond to Equation (33).

(c) Choose a suitable value of yield displacement for the oscillator.

(d) For $\hat{Q}_y$, subject the undamaged oscillator individually to each of the expected events and estimate the damage caused based on the representative PSDF of that event (see Appendix III). Find the maximum

of these damage estimates (across all the events expected). For each event, the properties of the equivalent linear oscillator are determined (see Appendix II) by increasing the calculated equivalent damping as in Equation (2).

(e) For $\bar{Q}_y$, subject the oscillator to all the expected events in a chosen sequence and estimate the maximum displacement and damage during each of the expected events by using the representative PSDF of that event (see Appendix III). Use these displacement and damage values to estimate the cumulative damage due to all the events in the sequence (see Appendix III). It may be noted that the yield displacement and stiffness of the damaged oscillator at the end of any event are estimated based on the damage caused during that event (see Appendix III), which then become the oscillator properties for the next event in the sequence. The properties of the equivalent oscillator during this event are determined (see Appendix II), while increasing the equivalent damping as in Equation (2).

(f) Iterate such that the chosen value of yield displacement gives the maximum damage (in the case of $\hat{Q}_y$) or cumulative damage (in the case of $\bar{Q}_y$) to be same as the target damage D.

(g) Multiply the iterated values of yield displacement with the stiffness of the oscillator to give $\hat{Q}_y$ and $\bar{Q}_y$.

Figure 13 shows the α_{RM} spectrum for the case considered in Figure 12. It may be observed that the DFR for multiplicity of events does not depend as much on the period of oscillator as the DFR proposed by Das et al. [10], and it may be possible to specify a single DFR for all oscillators (irrespective of their periods).

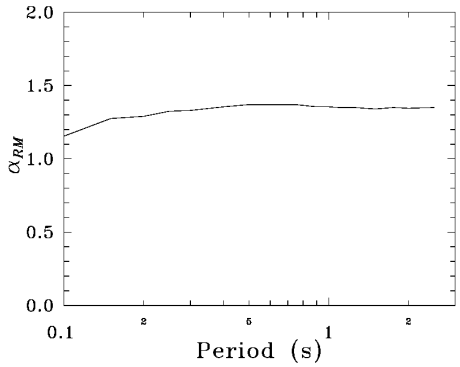

Fig. 13 DFR spectrum for multiplicity of events corresponding to the 'Proposed' DFR spectrum in Figure 12

In the following sub-sections, the dependence of α_{RM} spectrum on (a) the direction of residual displacement, (b) the sequencing of events, (c) the ductility capacity of the oscillator, and (d) the design life of the system under consideration is studied by considering D = 0.8 (with the assumption that D = 0.8 refers to the same limiting state of the system as considered for a ductility-based design).

2.1 Dependence on Direction of Residual Displacement

To study the dependence of α_{RM} spectrum on the direction of residual displacement, all the events are first arranged arbitrarily in the increasing order of their damage-causing potential. Those events which would not cause any damage are arranged in the increasing order of the maximum displacement caused by them in the undamaged structure. With this sequence of events remaining unchanged, seven combinations of directions of residual displacement after each event are considered as in Dey and Gupta [11]. Table 4 gives the events considered for residual displacement in the positive direction for these combinations, as represented by Cases I–VII. Each event in a combination is identified by the position in which it occurs in the assumed sequence.

Figure 14 shows the comparison of the α_{RM} spectra obtained for Cases I–VII for the seismic environment and oscillators considered for Figures 12–13. It may be observed that α_{RM} is sensitive to the

direction of residual displacement, with the maximum difference between the most critical and least critical cases being around 25% of α_{RM} for the least critical case. Case I, with all the residual displacements added up, gives the maximum values of α_{RM} and is the most critical case. On the other hand, Case II is the least critical case; here, the effect of positive residual displacement during an event is cancelled partially by the effect of negative residual displacement during the subsequent event. The extent of this cancellation however becomes less in Case III (due to the greater damage potential of latter events) and greater values of α_{RM} are obtained. It may be mentioned that greater sensitivity seen in the case of α_R by Dey and Gupta [11] is largely due to a different characterization of the anticipated motion; it is not due to the inherent differences between α_R and α_{RM}. On averaging over the initial period of the oscillator, a constant value of DFR for the multiplicity of events is obtained to be 1.33 and 1.10 for the most critical and the least critical cases, respectively.

Table 4: Events considered for residual displacement in positive direction under Cases I–VII

Case	Events for Residual Displacements in Positive Direction
I	1st, 2nd, 3rd, …, 47th
II	1st, 3rd, 5th, …, 47th
III	1st, 2nd, 5th, 6th, 9th, 10th, …, 45th, 46th
IV	1st, 4th, 7th, …, 46th
V	1st, 5th, 9th, …, 45th
VI	1st, 2nd, 4th, 5th, 7th, 8th, …, 46th, 47th
VII	1st, 2nd, 3rd, 5th, 6th, 7th, 9th, 10th, 11th, …, 45th, 46th, 47th

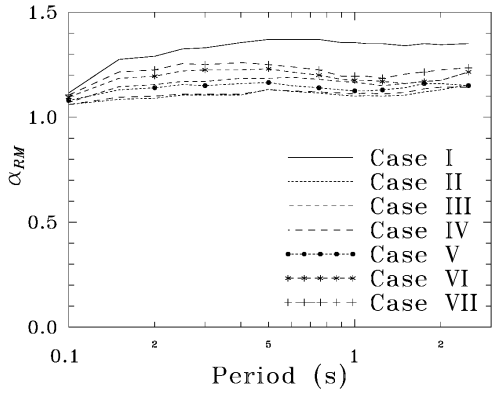

Fig. 14 Comparison of the modified DFR spectra (for multiplicity of events) for different combinations of the directions of residual displacements

2.2 Dependence on Sequencing of Events

To study the effect of the dependence of the sequencing of events on α_{RM} spectrum, the residual displacements after different events are assumed to be in the same direction (corresponding to the most critical case, Case I, as discussed above). Seven different sequences of events are considered as in Dey and Gupta [11], where the events in any sequence are identified by their rankings based on the damage that can be caused to the undamaged structure by each of them (or the maximum displacement that can be caused in the undamaged structure, if there are more than one events causing no damage). Thus, the event causing maximum damage is referred to as the 1st order event, and the event causing minimum damage is referred to as the 47th order event. Considering the specific situation of conventional design, where the cumulative damage is assumed to reach the damage state of collapse at the end of the most critical event, the 1st order event is placed at the end of each of the example sequences. Table 5 gives the order in which different events are assumed to occur for each example sequence.

Table 5: Details on order of event occurrence for example sequences A–G

Sequence	Order of Event Occurrence
A	2nd, 3rd, …, 47th, 1st Order
B	47th, 46th, 45th, …, 2nd, 1st Order
C	47th, 45th, 43rd, …, 3rd, 2nd, 4th, 6th, …, 46th, 1st Order
D	46th, 44th, 42nd, …, 2nd, 3rd, 5th, 7th, …, 47th, 1st Order
E	3rd, 5th, 7th, …, 47th, 46th, 44th, 42nd, …, 2nd, 1st Order
F	2nd, 4th, 6th, …, 46th, 47th, 45th, 43rd, …, 3rd, 1st Order
G	3rd, 4th, 7th, 8th, 11th, 12th, …, 43rd, 44th, 47th, 46th, 45th, 42nd, 41st, 38th, 37th, …, 6th, 5th, 2nd, 1st Order

Figure 15 shows the α_{RM} spectra for the seven sequences considered. The comparison of these spectra shows that α_{RM} has little sensitivity to the sequence of events, with the maximum variation with respect to the least critical case being just 5% and all seven curves overlapping with each other at long periods. On ignoring the dependence of α_{RM} on the period of the oscillator, α_{RM} may be assumed to be 1.33 for all the seven cases considered.

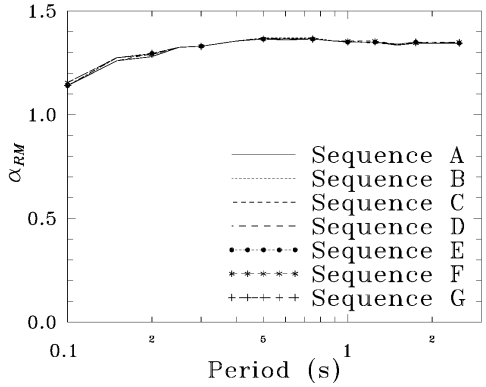

Fig. 15 Comparison of the modified DFR spectra (for multiplicity of events) for different sequences of the ordered events

2.3 Dependence on Ductility Capacity of Oscillator

Considering that the combination of (i) all residual displacements in the same direction (i.e., Case I) and (ii) all events arranged in the increasing order of their damage potential (i.e., Sequence B) is the most critical combination (among the cases considered), this is considered to study the dependence of α_{RM} spectra on the ductility capacity μ of the oscillator. Figure 16 shows the comparison of α_{RM} spectra for μ = 2.0, 2.5, and 3.0. It may be observed that α_{RM} increases with the ductility capacity of the oscillator, with oscillator period remaining unchanged. This is expected and consistent with the observations of Das et al. [10], since damage increases with ductility capacity of the oscillator and in order to keep it unchanged, the yield level has to be raised. At long periods, the effect of ductility capacity on α_{RM} is seen to be negligible, possibly due to the hysteretic energy contributing little to the damage in the case of flexible oscillators. At these periods, different α_{RM} appear to converge to the value of 1.35.

2.4 Dependence on Design Life of System

The combination of Case I and Sequence B is again considered to study the dependence of α_{RM} spectrum on the design life of the system. Figure 17 shows a comparison of the α_{RM} spectra for design life equal to 25, 50, and 75 yrs. As expected, α_{RM} increases with the design life of the system due to more events and thus greater damage in the system. On eliminating the (weak) dependence of α_{RM} on the

oscillator period, it is observed that α_{RM} goes up by 10%, if the design life is increased from 50 to 75 yrs and goes down by 15% in case the design life is decreased to 25 yrs.

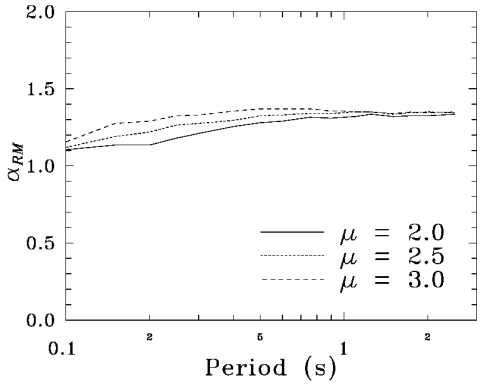

Fig. 16 Comparison of the modified DFR spectra (for multiplicity of events) for different values of ductility ratio

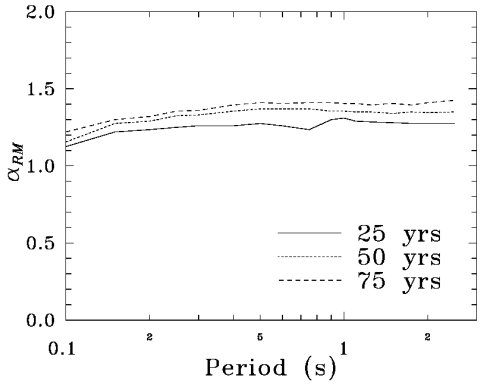

Fig. 17 Comparison of the modified DFR spectra (for multiplicity of events) for different values of design life

SUMMARY AND CONCLUSIONS

The formulation of Dey and Gupta [11] for estimating DFR spectrum for a given site in a seismic environment has been modified for an improved characterization of the seismic hazard at the site due to an earthquake event. The improvement relates to generalization of the spectrum-compatible PSDF considered by Dey and Gupta [11], so that it becomes applicable to the oscillators of a wide range of damping ratios. The proposed 'representative PSDF' is based on (a) a suitable increase in the damping of the oscillator (to account for the underdevelopment of steady-state oscillator response, due to the finite operating time of the excitation), such that there is minimum variation in the (spectrum-compatible) PSDFs obtained from the response spectra of different damping ratios, and (b) the averaging of the PSDFs so obtained. The proposed increase in oscillator damping depends on oscillator period and the strong-motion duration of excitation. This increase has been estimated for different definitions of strong-motion duration with the help of a suite of 225 motions recorded in western U.S.A. It has been illustrated through an example numerical study that the proposed representative PSDF, together with the statistical linearization of the oscillator response, can be used to reliably predict the response of elastic-perfectly-plastic oscillators.

The concept of DFR spectrum has been modified to reflect only the effects of multiplicity of events, while excluding the effects of shift from the conventional (ductility-based) design to a damage-based design. This has been done specifically for the situation where the most critical event occurs only after all the other events (expected during the design life of the structure) have occurred and the cumulative damage reaches the damage state of collapse at the end of the most critical event. The modified DFR spectrum is expected to estimate the raise required in the design yield force level of a SDOF structure in the conventional seismic design, such that the structure is able to survive the most critical event, even though no repairs have been carried out after the occurrence of smaller events. A numerical study based on a hypothetical seismic region of four faults and degrading elastic-perfectly-plastic oscillators has shown that the dependence of DFR on the initial period of the oscillator is weak, and thus a single value may be used to represent the DFRs for the oscillators of different periods.

A sensitivity analysis of the modified DFR spectrum has been carried out for various governing parameters like sequence of events, directions of residual displacements, ductility of the oscillator, and design life of the structure. It has been found that the sequence of events and directions of residual displacements do not significantly affect the proposed DFR spectrum. The most critical case is obtained for the residual displacements taking place in the same direction and different events occurring in the increasing order of their damage-causing potential. For such a situation, an increase of about 33% may need to be provided in the design yield force level for the structures of ductility capacity of 3 and design life of 50 years (in the case of the seismic environment considered in this study) to survive the most

critical event. It has been also observed that the modified DFR increases with the ductility capacity of the oscillator and with the design life of the structure, as seen in Das et al. [10] in the case of DFR.

It has been assumed in this study that a main shock is not followed by any aftershocks. It is possible that greater values of modified DFR are obtained on accounting for the contributions of aftershocks to the structural damage. Further, the methodology for the modified DFR spectrum needs to be extended to various other types of nonlinear oscillators for a more comprehensive treatment of the effects of multiplicity of events on the conventional seismic design.

APPENDIX I: MODIFICATION OF PSDF $G(\omega)$

Following is the procedure used by Dey and Gupta [11] to modify a given PSDF $G(\omega)$ to $\bar{G}(\omega)$ such that $\bar{G}(\omega)$ becomes compatible with a given set of (i) pseudo spectral acceleration (PSA) spectrum $\text{PSA}_{\text{target}}(T_n, \zeta)$ (for the SDOF oscillators of varying period T_n and fixed damping ratio ζ), and (ii) strong-motion duration T_s.

Using the stationary theory of random vibrations, the PSDF of the displacement response of a linear SDOF oscillator of period T_n and damping ratio ζ, which is excited at its base by the ground acceleration process of PSDF $G(\omega)$, is obtained as

$$S_x(\omega) = \left|H_x(\omega)\right|^2 G(\omega) \tag{8}$$

where

$$H_x(\omega) = \frac{-1}{\omega_n^2 - \omega^2 + 2\mathrm{i}\zeta\omega_n\omega} \tag{9}$$

denotes the transfer function relating the relative displacement of the oscillator mass to the base acceleration, i = $\sqrt{-1}$, and $\omega_n = 2\pi / T_n$. The response PSDF $S_x(\omega)$ is used to compute its moments, λ_0, λ_2 and λ_4, about the origin as

$$\lambda_n = \int_0^\infty \omega^n S_x(\omega)\mathrm{d}\omega; \quad n = 0, 2, 4 \tag{10}$$

which then leads to the following statistics of the absolute response process.

First, the root-mean-square (rms) value of the process is given by

$$|x|_{\text{rms}} = \sqrt{\lambda_0} \tag{11}$$

Second, the expected number of peaks is given by

$$\hat{N} = \frac{T_s}{2\pi}\left(1 + \sqrt{1-\varepsilon^2}\right)\left[\frac{\lambda_4}{\lambda_2}\right]^{1/2} \tag{12}$$

Third, the bandwidth parameter is given by

$$\varepsilon = \left[\frac{\lambda_0\lambda_4 - \lambda_2^2}{\lambda_0\lambda_4}\right]^{1/2} \tag{13}$$

Using these statistics, the expected amplitude of the i th order peak (in the absolute response process) is obtained as

$$E[|x|_{(i)}] = |x|_{\text{rms}} \int_0^\infty \eta\, p_{(i)}(\eta)\mathrm{d}\eta \tag{14}$$

where

$$p_{(i)}(\eta) = \frac{\hat{N}!}{(\hat{N}-i)!(i-1)!}\left[P(\eta)\right]^{i-1}\left[1-P(\eta)\right]^{\hat{N}-i} p(\eta) \tag{15}$$

is the probability function of the i th order peak. In Equation (15),

$$p(\eta)=\frac{\sqrt{2}}{\sqrt{\pi}(1+\sqrt{1-\varepsilon^2})}\left[\varepsilon e^{-\eta^2/2\varepsilon^2}+(1-\varepsilon^2)^{1/2}\eta e^{-\eta^2/2}\int_{-\infty}^{\eta(1-\varepsilon^2)^{1/2}/\varepsilon}e^{-x^2/2}\mathrm{d}x\right] \tag{16}$$

and

$$P(\eta)=\int_{\eta}^{\infty}p(u)\mathrm{d}u;\quad \eta\geq 0 \tag{17}$$

are the probability density and distribution functions, respectively, of the peaks in the absolute measure of the (relative) displacement response process. The expected amplitude of the largest peak, i.e., $\omega_n^2 E[|x|_{(1)}]$, is now compared with the value of the PSA spectrum ordinate of the oscillator, and $G(\omega)$ is modified to $\bar{G}(\omega)$ at $\omega=\omega_n$ such that

$$\bar{G}(\omega)|_{\omega=\omega_n}=G(\omega)|_{\omega=\omega_n}\left[\frac{\mathrm{PSA}_{\text{target}}(T_n,\zeta)}{\omega_n^2 E\left[|x|_{(1)}\right]}\right]^2 \tag{18}$$

By varying T_n suitably, $\bar{G}(\omega)$ is completely obtained. Finally, the computed $\bar{G}(\omega)$ is considered as $G(\omega)$ and the above steps are repeated to recalculate $\bar{G}(\omega)$. This is continued till the computed $\omega_n^2 E[|x|_{(1)}]$ becomes sufficiently close to $\mathrm{PSA}_{\text{target}}(T_n,\zeta)$ at all those values of T_n, for which the PSA spectrum has been specified.

APPENDIX II: PROPERTIES OF EQUIVALENT LINEAR OSCILLATOR

Following is the (iterative) procedure proposed by Caughey [19] for the calculation of the properties of an equivalent oscillator for a SDOF elastic-perfectly plastic oscillator of natural frequency ω_n, viscous damping ratio ζ, and yield displacement x_y, when it is subjected to the excitation process of the PSDF $G(\omega)$ at its base.

The natural frequency ω_e and damping ratio ζ_e of the equivalent oscillator are expressed as (Caughey [19])

$$\omega_e=\omega_n\sqrt{1-g(\sigma_y)} \tag{19}$$

and

$$\zeta_e=\frac{\zeta\omega_n}{\omega_e}+\frac{\omega_n^2}{\sqrt{2\pi}\omega_e^2\sigma_y}\left[1-\mathrm{erf}\left(\frac{1}{\sqrt{2}\sigma_y}\right)\right] \tag{20}$$

with

$$g(\sigma_y)=\frac{1}{2\pi\sigma_y^4}\int_1^{\infty}A^3\left(\pi-\Lambda+\frac{1}{2}\sin 2\Lambda\right)\exp\left(-\frac{A^2}{2\sigma_y^2}\right)\mathrm{d}A \tag{21}$$

$$\sigma_y=\frac{x_{\text{rms}}}{x_y} \tag{22}$$

and erf(.) representing the error function. Also, in Equation (22)

$$x_{\text{rms}}=\left[\int_0^{\infty}\left|\tilde{H}_x(\omega)\right|^2 G(\omega)\mathrm{d}\omega\right]^{1/2} \tag{23}$$

where

$$\tilde{H}_x(\omega)=\frac{-1}{\omega_e^2-\omega^2+2\mathrm{i}\zeta_e\omega_e\omega} \tag{24}$$

is the displacement transfer function for the equivalent oscillator under the base excitation. Further, Λ in Equation (21) is given by

$$\Lambda = \cos^{-1}\left(1-\frac{2}{A}\right) \tag{25}$$

An initial guess of σ_y is made, and the properties of the equivalent oscillator (i.e., ω_e and ζ_e) are calculated by using Equations (19)–(21). Corresponding to these properties, Equation (23) leads to a value of x_{rms}, which is then used to update σ_y via Equation (22). This process is repeated, until the updated value of σ_y differs from the previous value within a pre-specified tolerance.

APPENDIX III: COMPUTATION OF DFR SPECTRUM

Following are the details of the procedure used by Dey and Gupta [11] for the computation of DFR spectrum for a given seismic environment together with the location and properties of the nonlinear oscillator. In this procedure, $\bar{Q}_y$ and Q_y are obtained by first estimating the magnitudes of the likely events at each fault in the given seismic region, and then by estimating the power spectral density functions (PSDFs) of the likely ground motions due to those events. Next, for $\bar{Q}_y$, an appropriate sequence of events is chosen and the properties of the equivalent linear oscillator for each of the events are estimated by considering a suitable value of yield displacement x_y at the beginning of the event. This is followed by the estimation of the maximum and residual displacements during each of the events, and then by the estimation of the cumulative damage expected during the lifetime of the oscillator. If the cumulative damage is not equal to the target damage, the value of assumed yield displacement at the beginning of the first event is revised suitably. For Q_y, the estimation of PSDFs is followed by making an initial guess for the yield displacement x_y of the oscillator. Next, the properties of the equivalent linear oscillator are calculated and maximum displacement is estimated for each of the events corresponding to the chosen value of x_y. If the largest of the estimated maximum displacements together with the chosen yield displacement does not correspond to the maximum available ductility, the value of the chosen yield displacement is revised suitably.

1. Expected Magnitudes of Seismic Events

Assuming an exponential distribution of return period for a particular fault, with the known constants a and b, the expected number of events per year, N, exceeding the magnitude M at that fault is expressed as

$$\log N(M) = a - bM \tag{26}$$

This equation is used to estimate the expected number of earthquakes $\tilde{N}$ within the magnitude range from $M_{\min}$ = 5.0 to $M_{\max}$ = 8.0 during the lifetime of the oscillator. The expected magnitude of the ith largest event in the $\tilde{N}$ events is estimated as

$$E[M_i] = \int_{M_{\min}}^{M_{\max}} m p_i(m)\,\mathrm{d}m \tag{27}$$

where

$$p_i(m) = \frac{\tilde{N}!}{(\tilde{N}-i)!(i-1)!}[F(m)]^{i-1}[1-F(m)]^{\tilde{N}-i}\,p(m) \tag{28}$$

is the probability density function of the ith largest event, with

$$F(m) = \frac{10^{-b(m-M_{\min})} - 10^{-b(M_{\max}-M_{\min})}}{1-10^{-b(M_{\max}-M_{\min})}} \tag{29}$$

and

$$p(m) = b \ln 10 \frac{10^{-b(m-M_{\min})}}{1-10^{-b(M_{\max}-M_{\min})}} \tag{30}$$

Here, $F(m)$ and $p(m)$ are the probability distribution and density functions respectively of the $\tilde{N}$ events.

2. PSDF of Anticipated Ground Motion

The PSDF of the ground motion anticipated during an event of magnitude M_k occurring at the lth source is estimated as

$$G_{lk}(\omega) = \frac{\mathrm{PSV}_{lk}^2(\omega)}{\pi T_{lk}} \tag{31}$$

where $\mathrm{PSV}_{lk}(\omega)$ and T_{lk} respectively represent the PSV spectrum at frequency ω and strong-motion duration of the ground motion anticipated during the M_k-magnitude event at the lth fault. Dey and Gupta [11] did not specify the damping to which $\mathrm{PSV}_{lk}(\omega)$ corresponds. It is assumed here for convenience that $\mathrm{PSV}_{lk}(\omega)$ corresponds to the damping of the oscillator under consideration. This is estimated as (with $T_n = 2\pi/\omega$)

$$\log_{10} \mathrm{PSV}_{lk}(T_n) = M_k + \mathrm{Att}(\Delta_l, M_k, T_n) + b_1(T_n)M_k + b_2(T_n)s + b_5(T_n) + b_6(T_n)M_k^2 + \varepsilon(p, T_n) \tag{32}$$

where b_is represent the coefficients determined from a regression analysis at each period T_n; Δ_l is the representative distance from the lth source to the site, expressed in terms of the epicentral distance R_l, focal depth, fault size, and correlation radius of source function; s (= 0 for alluvium, 1 for intermediate, and 2 for rock) is the site geology parameter; $\mathrm{Att}(\Delta_l, M_k, T_n)$ represents the attenuation function for the M_k-magnitude event at the lth fault; and $\varepsilon(p, T_n)$ is the observed residual spectrum for the confidence level p = 0.5. The strong-motion duration T_{lk} is estimated as

$$T_{lk} = -4.88s + 2.33M_k + 0.149R_l \tag{33}$$

The PSDF estimated from Equation (31) is iteratively scaled up/down to $\bar{G}_{lk}(\omega)$ at different values of ω for compatibility with the pseudo spectral acceleration (PSA) spectrum corresponding to $\mathrm{PSV}_{lk}(T_n)$ (see Appendix I for the details of the procedure used).

3. Displacement Response of Nonlinear Oscillator

The largest, second largest, ... peaks in the displacement response of the (nonlinear) oscillator (with period T_n at the beginning of the excitation) under consideration are estimated for the PSDF $\bar{G}_{lk}(\omega)$ by first finding the natural frequency ω_e and damping ratio ζ_e of the equivalent linear oscillator as described in Appendix II. The PSDF $E_{lk}(\omega)$ of the displacement response process is then calculated as

$$E_{lk}(\omega) = \left|\tilde{H}_x(\omega)\right|^2 \bar{G}_{lk}(\omega) \tag{34}$$

where $\tilde{H}_x(\omega)$ is the transfer function of the displacement response of the equivalent linear oscillator as in Equation (24).

With $E_{lk}(\omega)$ taken as $S_x(\omega)$ and T_{lk} as T_s, the procedure described in Appendix I (see Equations (10)–(17)) is used to estimate the expected ith order peak in the absolute displacement response, i.e., $E[|x|_{(i)}]$. The same procedure is used to estimate the expected ith order peak in the displacement response process, i.e., $E[x_{(i)}]$, but in this case $p(\eta)$ and $\hat{N}$ are instead considered as

$$p(\eta)=\frac{1}{\sqrt{2\pi}}\left[\varepsilon e^{-\eta^2/2\varepsilon^2}+(1-\varepsilon^2)^{1/2}\eta e^{-\eta^2/2}\int_{-\infty}^{\eta(1-\varepsilon^2)^{1/2}/\varepsilon}e^{-x^2/2}\mathrm{d}x\right] \tag{35}$$

and

$$\hat{N}=\frac{T_{lk}}{2\pi}\left[\frac{\lambda_4}{\lambda_2}\right]^{1/2} \tag{36}$$

The magnitude of the residual displacement R_d (at the end of the excitation) is estimated as

$$|R_d|=(\alpha+\beta/T_n^{\gamma})E[|x|_{(1)}] \tag{37}$$

where the values of the constants α, β, and γ are same as specified in Harikrishnan and Gupta [31] for the $C_{r,i}(T)$ spectrum. The sign of the residual displacement is random and needs to be assumed.

4. Cumulative Damage during Lifetime

In order to estimate the cumulative damage during the lifetime of the oscillator under consideration for a given sequence of n_e events, the properties of the oscillator at the beginning of the i th event are modified based on the additional damage in the oscillator due to the $(i-1)$ th event. Assuming that $\hat{D}_i$ denotes the (additional) damage in the oscillator due to the i th event, the stiffness of the oscillator at the end of the i th event is taken as

$$k_{i+1}=k_i\left[1-\hat{D}_i\right]^{0.1};\quad 1\le i<n_e \tag{38}$$

with $k_1\equiv k$ representing the initial stiffness of the oscillator. The yield displacement at the end of the i th event is taken as

$$x_{y,i+1}=x_{y,i}\left(\frac{k_1+k_i}{k_1+k_{i+1}}\right) \tag{39}$$

with $x_{y,1}\equiv x_y$. The stiffness and yield displacement of the oscillator at the end of the i th event are assumed to remain unchanged till the beginning of the $(i+1)$ th event.

The additional damage $\hat{D}_i$ inflicted on the oscillator during the i th event of the assumed sequence is estimated as

$$\hat{D}_i=\hat{D}_{i,\mathrm{displ}}+D_{i,\mathrm{energy}} \tag{40}$$

where $\hat{D}_{i,\mathrm{displ}}$ and $D_{i,\mathrm{energy}}$ respectively are the maximum displacement-based and energy-based damage terms corresponding to the i th event. Those are estimated as (for $i\ge 2$)

$$\hat{D}_{i,\mathrm{displ}}=\frac{x'_{m,i}-x_{y,i}}{x_u-x_{y,i}}-\sum_{j=1}^{i-1}\hat{D}_{j,\mathrm{displ}}\ \text{or zero, whichever is greater} \tag{41}$$

with

$$\hat{D}_{1,\mathrm{displ}}=\frac{x_{m,1}-x_y}{x_u-x_y} \tag{42}$$

and

$$D_{i,\mathrm{energy}}=\beta\frac{E_{H,i}}{F_{y,i}x_u} \tag{43}$$

where, $F_{y,i}=k_i x_{y,i}$, $x_u=\mu x_y$, and $\beta=0.1$. Here,

$$x'_{m,i} = \left| \sum_{j=1}^{i-1} R_{d,j} - x_{m,i} + R_{d,i} \right| \text{ or } \left| \sum_{j=1}^{i-1} R_{d,j} + x_{m,i} \right|, \text{ whichever is greater, for } R_{d,i} > 0 \quad (44)$$

and

$$x'_{m,i} = \left| \sum_{j=1}^{i-1} R_{d,j} - x_{m,i} \right| \text{ or } \left| \sum_{j=1}^{i-1} R_{d,j} + x_{m,i} + R_{d,i} \right|, \text{ whichever is greater, for } R_{d,i} < 0 \quad (45)$$

describe the maximum absolute displacement in the oscillator during the i th event (after it is modified to include the effect of residual displacement), with $R_{d,i}$ representing the residual displacement due to the i th event and $x_{m,i}$ being same as $E[|\, x\,|_{(1)}]_i$. Further,

$$E_{H,i} = \sum_{s=1}^{N_0} 4(E[x_{(s)}]_i - x_{y,i}) k_i x_{y,i} \quad (46)$$

represents the total hysteretic energy dissipated during the i th event, where N_0 is the number of peaks in the displacement process with amplitudes exceeding $x_{y,i}$ during this event, and $E[x_{(s)}]_i$ denotes the s th order peak in the displacement process during the i th event.

REFERENCES

1. Bozorgnia, Y. and Bertero, V.V. (editors) (2004). "Earthquake Engineering: From Engineering Seismology to Performance-Based Engineering", *CRC Press, Boca Raton, U.S.A.*
2. Elnashai, A.S., Bommer, J.J. and Martinez-Pereira, A. (1998). "Engineering Implications of Strong-Motion Records from Recent Earthquakes", *Proceedings of the 11th European Conference on Earthquake Engineering, Paris, France (on CD).*
3. Decanini, L., Gavarini, C. and Mollaioli, F. (2000). "Some Remarks on the Umbria-Marche Earthquakes of 1997", *European Earthquake Engineering, Vol. XIV, No. 3, pp. 18–48.*
4. Amadio, C., Fragiacomo, M. and Rajgelj, S. (2003). "The Effects of Repeated Earthquake Ground Motions on the Non-linear Response of SDOF Systems", *Earthquake Engineering & Structural Dynamics, Vol. 32, No. 2, pp. 291–308.*
5. Moustafa, A. and Takewaki, I. (2011). "Response of Nonlinear Single-Degree-of-Freedom Structures to Random Acceleration Sequences", *Engineering Structures, Vol. 33, No. 4, pp. 1251–1258.*
6. Hatzigeorgiou, G.D. and Beskos, D.E. (2009). "Inelastic Displacement Ratios for SDOF Structures Subjected to Repeated Earthquakes", *Engineering Structures, Vol. 31, No. 11, pp. 2744–2755.*
7. Hatzigeorgiou, G.D. (2010). "Ductility Demand Spectra for Multiple Near- and Far-Fault Earthquakes", *Soil Dynamics and Earthquake Engineering, Vol. 30, No. 4, pp. 170–183.*
8. Hatzigeorgiou, G.D. and Liolios, A.A. (2010). "Nonlinear Behaviour of RC Frames under Repeated Strong Ground Motions", *Soil Dynamics and Earthquake Engineering, Vol. 30, No. 10, pp. 1010–1025.*
9. Das, S. and Gupta, V.K. (2022). "On Contribution of Aftershocks to Cumulative Seismic Damage in RC Frames", *ISET Journal of Earthquake Technology, Vol. 59, No. 1, pp. 1–26*.
10. Das, S., Gupta, V.K. and Srimahavishnu, V. (2007). "Damage-Based Design with No Repairs for Multiple Events and Its Sensitivity to Seismicity Model", *Earthquake Engineering & Structural Dynamics, Vol. 36, No. 3, pp. 307–325.*
11. Dey, P. and Gupta, V.K. (2020). "Effect of Residual Displacement and Sequence of Events on Design Force Ratio Spectrum", *Soil Dynamics and Earthquake Engineering, Vol. 131, Paper 105974.*
12. Shrikhande, M. and Gupta, V.K. (1997). "A Generalized Approach for the Seismic Response of Structural Systems", *European Earthquake Engineering, Vol. XI, No. 2, pp. 3–12.*
13. Kaul, M.K. (1978). "Stochastic Characterization of Earthquakes through Their Response Spectrum", *Earthquake Engineering & Structural Dynamics, Vol. 6, No. 5, pp. 497–509.*

14. Unruh, J.F. and Kana, D.D. (1981). "An Iterative Procedure for the Generation of Consistent Power/Response Spectrum", *Nuclear Engineering and Design, Vol. 66, No. 3, pp. 427–435.*
15. Christian, J.T. (1989). "Generating Seismic Design Power Spectral Density Functions", *Earthquake Spectra, Vol. 5, No. 2, pp. 351–368.*
16. Gupta, I.D. and Trifunac, M.D. (1998). "Defining Equivalent Stationary PSDF to Account for Nonstationarity of Earthquake Ground Motion", *Soil Dynamics and Earthquake Engineering, Vol. 17, No. 2, pp. 89–99.*
17. Dey, A. and Gupta, V.K. (1998). "Response of Multiply Supported Secondary Systems to Earthquakes in Frequency Domain", *Earthquake Engineering & Structural Dynamics, Vol. 27, No. 2, pp. 187–201.*
18. Sethi, H. (2012). "Effect of Multiple Events with No Repairs on Ductility-Based Seismic Design", *M.Tech. Thesis, Department of Civil Engineering, Indian Institute of Technology Kanpur, Kanpur*.
19. Caughey, T.K. (1960). "Random Excitation of a System with Bilinear Hysteresis", *Journal of Applied Mechanics, ASME, Vol. 27, No. 4, pp. 649–652.*
20. Caughey, T.K. and Stumpf, H.J. (1961). "Transient Response of a Dynamic System under Random Excitation", *Journal of Applied Mechanics, ASME, Vol. 28, No. 4, pp. 563–566.*
21. Rosenblueth, E. and Elorduy, J. (1969). "Responses of Linear Systems to Certain Transient Disturbances", *Proceedings of the Fourth World Conference on Earthquake Engineering, Santiago, Chile, Vol. 1, pp. A-1-185–A-1-196.*
22. Ambraseys, N.N. and Sarma, S.K. (1967). "The Response of Earth Dams to Strong Earthquakes", *Geotechnique, Vol. 17, No. 3, pp. 181–213.*
23. Murphy, J.R. and O'Brien, L.J. (1977). "The Correlation of Peak Ground Acceleration Amplitude with Seismic Intensity and Other Physical Parameters", *Bulletin of the Seismological Society of America, Vol. 67, No. 3, pp. 877–915.*
24. Sarma, S.K. and Casey, B.J. (1990). "Duration of Strong Motion in Earthquakes", *Proceedings of the Ninth European Conference on Earthquake Engineering, Moscow, U.S.S.R., Vol. 10-A, pp. 174–183.*
25. McCann, Jr., M.W. and Shah, H.C. (1979). "Determining Strong-Motion Duration of Earthquakes", *Bulletin of the Seismological Society of America, Vol. 69, No. 4, pp. 1253–1265.*
26. Trifunac, M.D. and Brady, A.G. (1975). "A Study on the Duration of Strong Earthquake Ground Motion", *Bulletin of the Seismological Society of America, Vol. 65, No. 3, pp. 581–626.*
27. Vanmarcke, E.H. and Lai, S.S.P. (1980). "Strong-Motion Duration and RMS Amplitude of Earthquake Records", *Bulletin of the Seismological Society of America, Vol. 70, No. 4, pp. 1293–1307.*
28. Samdaria, N. and Gupta, V.K. (2018). "A New Model for Spectral Velocity Ordinates at Long Periods", *Earthquake Engineering & Structural Dynamics, Vol. 47, No. 1, pp. 169–194.*
29. Lee, V.W. and Trifunac, M.D. (1987). "Strong Earthquake Ground Motion Data in EQINFOS: Part 1", *Report CE 87-01, University of Southern California, Los Angeles, U.S.A.*
30. Park, Y.J. and Ang, A.H.S. (1985). "Mechanistic Seismic Damage Model for Reinforced Concrete", *Journal of Structural Engineering, ASCE, Vol. 111, No. 4, pp. 722–739.*
31. Harikrishnan, M.G. and Gupta, V.K. (2020). "Scaling of Residual Displacements in Terms of Elastic and Inelastic Spectral Displacements for Existing SDOF Systems", *Earthquake Engineering and Engineering Vibration, Vol. 19, No. 1, pp. 71–85.*